Fusion cross section of the $^{16}O+^{13}C$ reaction

C. T. Papadopoulos, R. Vlastou, and E. N. Gazis
National Technical Univeristy of Athens, Athens 157 73, Greece

P. A. Assimakopoulos
The University of Ioannina, Ioannina 453 32, Greece

C. A. Kalfas, S. Kossionides, and A. C. Xenoulis
Nuclear Research Centre Demokritos, Aghia Paraskevi Attikis 153 10, Greece
(Received 2 December 1985)

Individual evaporation channels and total fusion cross sections have been deduced for the $^{16}O + ^{13}C$ reaction in the center of mass energy range 7.8—14.6 MeV. This was accomplished through measurements of absolute γ-ray yields from low-lying levels of evaporation residues. Singles γ-ray spectra were obtained with a high resolution Ge(Li) detector at an angle $\theta_\gamma = 125°$ with respect to the ^{16}O beam. All excitation functions measured are devoid of any structure, in contrast with the well-known oscillations observed in $^{16}O + ^{12}C$. The results are compared to statistical model calculations and predictions of macroscopic models.

I. INTRODUCTION

Even though the general characteristics of the fusion process for light-heavy nuclei may be adequately described using macroscopic models,[1–4] certain details of the energy dependence of the cross section near and above the Coulomb barrier still lack description and understanding. Such fusion reactions have thus attracted in recent years a great deal of experimental and theoretical efforts.[5–19] In particular the well-established occurrence of wide oscillations in the fusion excitation function, observed for 0^+, α-cluster-type systems,[6–11] such as $^{12}C + ^{12}C$, $^{16}O + ^{16}O$, and $^{12}C + ^{16}O$, and its disappearance in other systems, is still a matter of investigation. In this context it is conjectured that the addition of one extra nucleon, outside the α-cluster core, in one of the interacting nuclei induces a radically different behavior in the fusion excitation function.[7] It is evident that such behavior cannot be accounted for by any type of macroscopic model and that more microscopic models taking into account the detailed structure of the interacting nuclei should be employed.

To elucidate the influence of one or two additional nucleons outside an α-cluster core on the fusion cross section several systems such as[12–18] $^{12}C + ^{13}C$, $^{16}O + ^{17}O$, $^{17}O + ^{12}C$, $^{12}C + ^{14}C$, and $^{12}O + ^{18}O$, have been experimentally investigated. The general trend in these systems is an enhancement of the cross section with respect to the fusion of the bare α-cluster cores, while resonances observed in the excitation function of the corresponding α-cluster cores dissappear or are significantly reduced. No similar trend has been established for these systems, in other channels such as inelastic scattering or single nucleon transfer.

In the present work the partial and total fusion cross sections in the $^{16}O + ^{13}C$ reaction have been measured in the 7.8—14.6 MeV center of mass energy range, which straddles the Coulomb barrier region. Limited experimental investigations of this system have been previously reported in the literature. Chan *et al.*[19] have measured the excitation function of the 585 keV γ ray in the evaporation channel leading to ^{25}Mg up to 25 MeV center of mass energy. In the same energy range Freeman[13] has also reported similar measurements, which, however, disagree both with respect to the magnitude and the structure of the evaporation cross section. More recently Dasmahapatra *et al.*[20] have measured the total fusion cross section at energies (4.6—9.1 MeV) below the Coulomb barrier, confirming a marked enhancement over the $^{16}O + ^{12}C$ cross section in accordance with the expected attractive action of the loosely bound neutron in the ^{13}C nucleus. The purpose of the present experiment is to extend the investigation of this system at energies well above the Coulomb barrier.

II. EXPERIMENTAL PROCEDURE

The ^{16}O beam was obtained from the *T*11/25 tandem Van de Graaff accelerator of the Nuclear Research Center Democritos and was deflected into a *D*-shaped scattering chamber containing the ^{13}C target. The size of the beam was defined by two tantalum collimators of 2 mm aperture placed at 70 cm and 135 cm from the target. To avoid carbon buildup on the target the beam entered the chamber through a 14 cm long aluminum tube maintained at liquid nitrogen temperature. The target was composed of a 110 $\mu g/cm^2$ ^{13}C layer (98.9% iostropic purity) evaporated onto a 100 mg/cm^2 Au backing. The backing ensured complete stopping of the beam in the target and was necessary both for effective beam-current monitoring and for reducing the large γ-ray Doppler broadening. To ensure the accuracy of beam-current measurements the target was surrounded by a cylindrical tantalum shroud with a 1.5 cm entrance aperture, which was biased at -300 V

relative to local ground.

Singles γ-ray spectra were obtained with an adequately shielded 95 cm^3 Ge(Li) detector at 15 cm from the target and at an angle of 125° with respect to the beam direction. Since the second order Legendre polynomial P_2 vanishes at 125°, these spectra were assumed to represent angle-integrated yields. In addition, the considerable Doppler shift at this angle allowed a separation between prompt and delayed (from β decay) components of several γ rays. At 27 MeV incident ^{16}O energy some spectra were also taken at 90° and 55° with respect to the beam in order to help identification of certain γ rays.

Singles 125° γ-ray spectra were taken in the range of 18—33 MeV incident ^{16}O energy (7.8 to 14.6 MeV center of mass energy, if the appropriate energy loss in the target is taken into account) in 0.5 MeV (0.22 MeV center of mass) steps in a 100 h continuous run. Carbon buildup on the target during this period was carefully monitored by collecting a 27 MeV spectrum every twelve hours. The intensity of certain peaks in these monitor spectra, contaminated by the $^{16}O + ^{12}C$ reaction, was then compared to the corresponding 279 keV peak from the ^{197}Au backing. It was determined in this manner that ^{12}C contamination at the end of the overall run period reached a level of the order of 5%.

The relative efficiency curve of the Ge(Li) detector was determined from ^{56}Co and ^{152}Eu spectra taken under identical experimental conditions. The final absolute efficiency curve was determined by using a standard calibrated ^{60}Co source. Normalization of the 125° spectra through the energy region covered in the experiment was affected both with the integrated current (and electronic dead time) and with the observed yield of the Au 279 keV γ ray. For this purpose the Coulomb excitation cross section for this line was calculated according to the thick-target semiclassical theory of Alder *et al.*[21] The γ ray branching ratio of the 279→0 keV transition, as well as the $B(E2)$ strength and internal conversion coefficient values used in the calculation were taken from Ref. 22.

To evaluate the contribution of β decay, an electronic unit was used which automatically switched the beam "on" and "off" successively for short periods, while directing the data to different analog-to-digital converters (ADC's). This procedure was repeated at the end of each run, for several of the beam energies with "beam on" and "beam off" times appropriate for the half-life of the γ rays under investigation.

III. REDUCTION OF EXPERIMENTAL DATA

The exit channels of the $^{16}O + ^{13}C$ reaction are arranged according to their binding energy in Fig. 1. Figure 2 contains a typical γ-ray pulse height spectrum obtained at 27 MeV ^{16}O laboratory energy and at an angle $\theta_\gamma = 125°$ with respect to the beam direction. Prominent gamma lines emitted by the residual nuclei, following light particle evaporation, are summarized in Table I.

As already mentioned, since many residual nuclei may also be reached through the $^{16}O + ^{12}C$ entrance channel, the observed yields of certain γ rays had to be corrected for initial contamination (1%) and subsequent buildup of

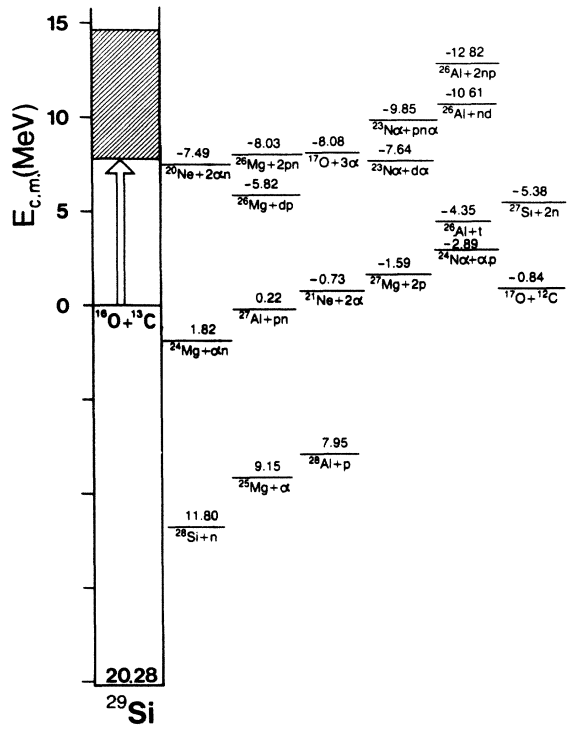

FIG. 1. Energy diagram for exit channels of the $^{16}O + ^{13}C$ reaction. The cross-hatched area indicates the excitation energy in the compound nucleus ^{29}Si explored in the present study. Values of ground-state Q values are given in MeV.

carbon on the target. This was particularly important in the case of the three-particle exit channels listed in Fig. 1. This was accomplished by subtracting the linear ^{12}C accumulation (from 1% to 5%) observed during the run. To estimate the $^{16}O + ^{12}C$ contribution to individual γ rays the absolute cross sections measured by Chan *et al.*[11] were employed.

The cross section $\sigma_{res}(k)$ corresponding to the formation of a residual nucleus k is obtained from the cross section $\sigma_\gamma(k,i)$ of a γ ray i emitted by this nucleus through

$$\sigma_{res}(k) = \frac{\sigma_\gamma(k,i)}{F_{ki}} \tag{1}$$

where F_{ki} is the summing and branching factor[23] determined by statistical model calculations. This factor takes into account both the contribution of a particular γ-ray i to the total cross section in channel k and contributions due to summing of γ rays in the detector. It should be pointed out, however, that the latter effect was negligible in the present experiment due to the large target-to-detector distance.

In the present research the factors F_{ki} were calculated by using a modified version of the statistical model code STAPRE,[24] which is designed to estimate energy-averaged cross sections for particle-induced reactions with several emitted particles (n,p,α,d) and γ rays under the assumption of sequential evaporation. Discrete energy levels and branching ratios, required as input in the statistical model

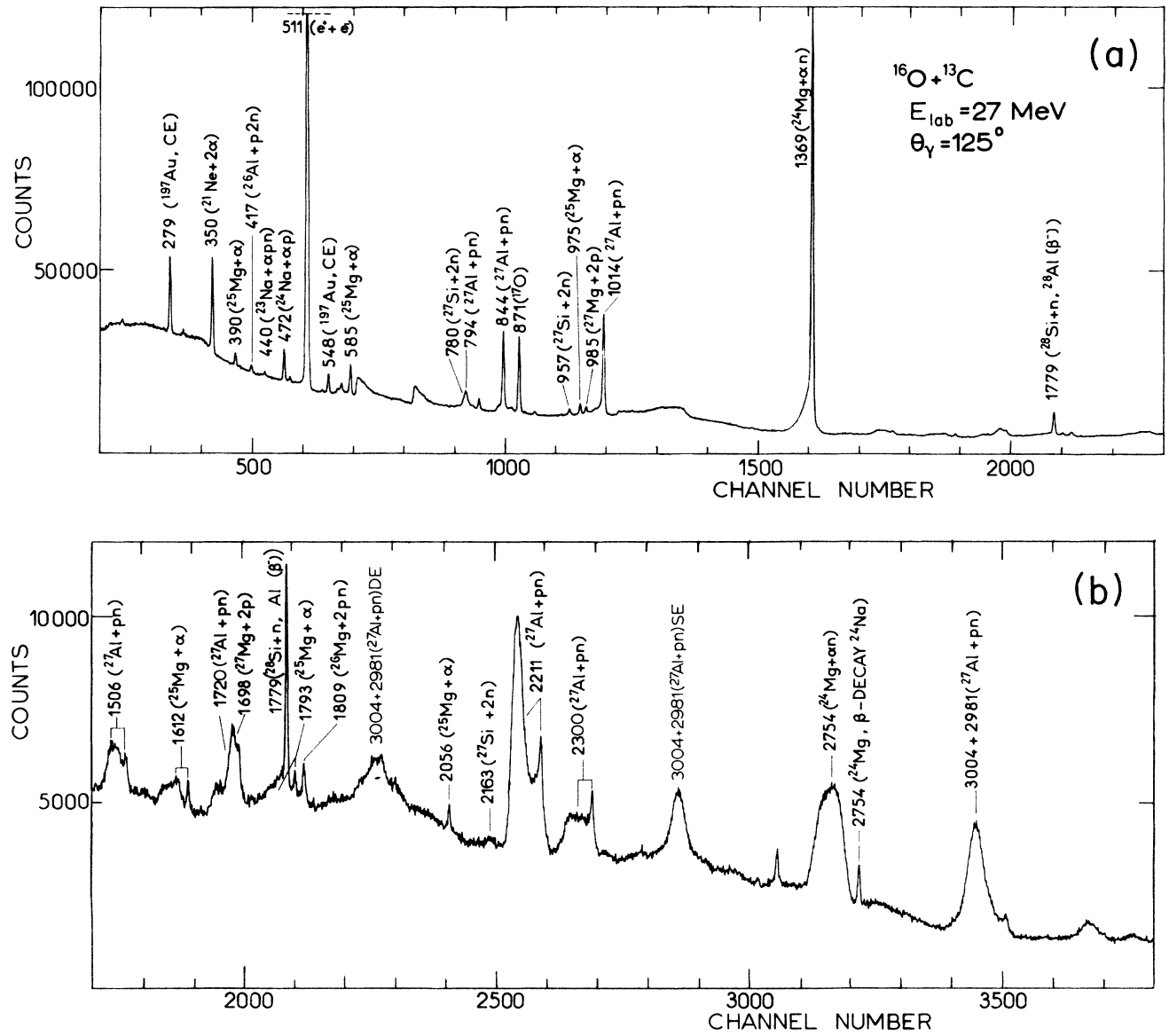

FIG. 2. Gamma-ray pulse height spectrum from the $^{16}O + ^{13}C$ reaction at 27 MeV ^{16}O bombarding energy and angle of observation $\theta_\gamma = 125°$. The energy and origin of individual photopeaks are indicated in the figure.

code, were taken from Ref. 25. For the density of levels in the continuum the back-shifted Fermi gas model with equidistant levels[26] assuming the Lang formula,[27] was used. The parameters entering this model are the single particle level density α, the fictive ground state position Δ, and the effective moment of inertia θ_{eff}, related to the rigid rotor estimate θ_{rig} through the expression $\theta_{\text{eff}} = \eta\theta_{\text{rig}}$. The values of the parameters used here are summarized in Table II.

Transmission coefficients for emitted light particles were obtained from optical model calculations using parameters proposed in the literature for neutrons,[28] protons,[29] deuterons,[30] and alphas.[31] The entrance channel transmission coefficients $T_l(E)$ were calculated according to Eqs. (3) and (4) below. These were obtained by considering the parameters R_{Bl} and ω_l independent of l ($R_{Bl} = R_B$, $\omega_l = \omega$). Numerical values of V_B and R_B were chosen so that they reproduced the fusion cross section $^{16}O + ^{13}C$ data obtained by Dasmahapatra *et al.*[20] in the energy range 7.5–9.1 MeV, which evince the characteristic $1/E$ dependence. The calculation of the final cross section was found to be sensitive to the parameter ω only in a small region at the low energy tail, adjacent to the Coulomb barrier. Therefore $\hbar\omega = 3$ MeV was employed as an initial value for the whole energy range considered in this experiment.

In order to reduce the experimental data according to Eq. (1), reliable values of F factors are required. For this reason an extensive investigation was undertaken with regards to the influence of each parameter entering the sta-

TABLE I. Prominent γ rays observed in the reaction $^{16}O + ^{13}C$.

Exit channel: Residual nucleus	Light particles	Transitions E_γ (keV) $J_i^\pi \rightarrow J_f^\pi$					
^{28}Si	n	1779 $2^+ \rightarrow 0^+$					
^{28}Al	p	940 $0^+ \rightarrow 2^+$					
^{25}Mg	α	585 $\frac{1}{2}^+ \rightarrow \frac{5}{2}^+$,	975 $\frac{3}{2}^+ \rightarrow \frac{5}{2}^+$,	390 $\frac{3}{2}^+ \rightarrow \frac{1}{2}^+$,	1612 $\frac{7}{2}^+ \rightarrow \frac{5}{2}^+$,	1793 $\frac{9}{2}^+ \rightarrow \frac{7}{2}^+$,	2056 $\frac{13}{2}^+ \rightarrow \frac{9}{2}^+$
^{27}Si	nn	780 $\frac{1}{2}^+ \rightarrow \frac{5}{2}^+$,	957 $\frac{3}{2}^+ \rightarrow \frac{5}{2}^+$,	2163 $\frac{7}{2}^+ \rightarrow \frac{5}{2}^+$			
^{27}Mg	pp	985 $\frac{3}{2}^+ \rightarrow \frac{1}{2}^+$,	1698 $\frac{5}{2}^+ \rightarrow \frac{1}{2}^+$				
^{27}Al	pn/d	844 $\frac{1}{2}^+ \rightarrow \frac{5}{2}^+$,	1014 $\frac{3}{2}^+ \rightarrow \frac{5}{2}^+$,	2211 $\frac{7}{2}^+ \rightarrow \frac{5}{2}^+$,	1720 $\frac{5}{2}^+ \rightarrow \frac{3}{2}^+$,	2981 $\frac{3}{2}^+ \rightarrow \frac{5}{2}^+$	
		3004 $\frac{9}{2}^+ \rightarrow \frac{5}{2}^+$,	794 $\frac{9}{2}^+ \rightarrow \frac{7}{2}^+$,	2300 $\frac{11}{2}^+ \rightarrow \frac{7}{2}^+$,	1506 $\frac{11}{2}^+ \rightarrow \frac{9}{2}^+$		
^{24}Mg	αn	1369 $2^+ \rightarrow 0^+$,	2754 $4^+ \rightarrow 2^+$				
^{24}Na	αp	472 $1^+ \rightarrow 4^+$					
^{21}Ne	$\alpha\alpha$	350 $\frac{5}{2}^+ \rightarrow \frac{3}{2}^+$					
^{26}Al	nnp/nd/t	417 $3^+ \rightarrow 5^+$					
^{26}Mg	ppn/pd	1809 $2^+ \rightarrow 0^+$					
^{23}Na	αpn/αd	440 $\frac{5}{2}^+ \rightarrow \frac{3}{2}^+$					
^{20}Ne	$\alpha\alpha$n	1634 $2^+ \rightarrow 0^+$					
^{17}O	3α or n transfer	871 $\frac{1}{2}^+ \rightarrow \frac{5}{2}^+$					

tistical model calculations.

As pointed out in Ref. 32 the influence of transmission coefficients for light particle emission on the F factors is less than 3%. This dependence therefore was not further considered in the present investigation. Similarly, in order to investigate the influence of entrance channel transmission coefficients, F factors were calculated both through the method described above and optical model calculations. In the first case values of $\hbar\omega = 3$ and 5 MeV were tried which produced less than 3% variations in F-factor values. In the latter calculations, the parameters contained in Table IV, obtained by fitting elastic scattering data (see Sec. V below), were employed. Values of F factors resulting from the two methods of calculation were seen to agree within 3%.

TABLE II. Level density parameters used in the Hauser-Feshbach calculations.

Nucleus	α (MeV^{-1})	Δ (MeV)	Reference
^{28}Si	3.00	2.00	26
^{28}Al	3.40	−2.50	34
^{27}Si	3.08	−0.14	23
^{27}Mg	3.30	0.43	34
^{27}Al	3.30	0.43	23
^{26}Al	3.40	−1.24	34
^{26}Mg	3.47	0.60	33
^{25}Mg	3.13	−1.40	32
^{24}Mg	2.79	2.10	32
^{23}Na	2.88	−1.00	32
^{21}Ne	3.00	−0.90	32
^{20}Ne	2.67	2.00	32

The variation of F factors with respect to the Fermi model parameters α, Δ, and η was also investigated. Several tests were conducted by using different sets of values of α and Δ taken from the literature with $\eta = 1$. For most of the residual nuclei the F factors for γ rays employed in the calculations were affected by less than 3% with the exception of ^{25}Mg, where variations of up to 20% appeared for certain transitions. Several values of the parameter η, which affects the spin density distribution, were also tested. In the range of 0.8–1.0 several values of η, which reproduced the position of high spin states at high excitation energy, were tried. As a result of this investigation it was found that the F factors for high spin states changed drastically, while for low spin states they remained almost unaffected. It should be noted that the above range of variation in the Fermi model parameters, although producing substantial differences in the calculated cross sections of the residual nuclei, affect the corresponding values of F factors to a much lesser degree.

The final set of Fermi model parameters employed here are summarized in Table II and were taken from the references also included in the table. Summing and branching ratios calculated with this set of values are plotted in Fig. 3. The uncertainties in the F factors determined through the previous analysis were included in the value of the corresponding cross sections calculated using Eq. (1). The resulting errors ranged between 5% and 10%.

As a further test on the consistency of the results and, in particular, the reliability of calculated summing and branching factors entering Eq. (1), the ratio $R = 2\sigma_i/(\sigma_i + \sigma_j)$ of cross sections σ_i and σ_j deduced from two different γ rays i and j, deexciting a given nu-

cleus, were examined. Examples of such an investigation for ^{27}Al and ^{25}Mg are contained in Fig. 4 and reveal a deviation of this ratio from the expected value of unity by less than 10%.

Finally the accuracy of calculated F factors was tested by evaluating the cross section for populating a particular nucleus from its subsequent β decay. An example of such a measurement for ^{27}Mg, observed through the 844 and 1014 keV transitions in ^{27}Al, is included in Fig. 6 (open circles) and agrees within experimental errors, with the cross section obtained through Eq. (1) (filled circles).

IV. EXPERIMENTAL RESULTS

Prominent γ rays employed to extract cross sections for individual exit channels are underlined in Table I. In addition to good statistics in the γ-ray spectra these transitions were also selected for their moderate to high summing and branching factors. Several weaker γ rays or transitions with abnormally low F factors, which nevertheless aided the analysis, are also included in Table I.

The results obtained in this analysis are discussed in some detail below.

A. One particle evaporation channels

These channels contribute approximately 10% to the total fusion cross section at low energies and less than 4% at the higher energies covered in this experiment, mainly due to their high Q values. All three channels are free of contamination from the ^{16}O + ^{12}C reaction.

From separate radioactivity measurements it was determined that the main contribution to the 1779 keV transition in ^{28}Si comes from the β decay of ^{28}Al ($T_{1/2}=2.24$ min). This contribution varies from 90% at low energies to almost 100% at 33 MeV. To test this result the cross section for populating the ^{28}Al + p channel had to be calculated from the ^{28}Al γ rays. Unfortunately the most prominent transitions in ^{28}Al (1014 and 983 keV) could not be adequately resolved in the spectra and the only available γ ray was the weak 942 keV transition. Although the F factor for this transition is very low (0.02–0.06) the deduced cross section agreed very well with the β-decay result. It was therefore decided to add the ^{28}Al + p cross sections, as extracted from the 1779 keV transition, to the total fusion cross section. It should be noted in this context that even in the extreme case that the 1779 keV γ ray is attributed entirely to ^{28}Si, its contribution to the total fusion cross section would remain unchanged within 1%, since the corresponding F factor (for ^{28}Si) varies between 0.80 and 0.94. The cross section deduced for the 1779 keV transition is shown in Fig. 5.

Population of the ^{25}Mg + α exit channel could be observed from several γ rays listed in Table I and shown in Fig. 5. The value adopted for formation of ^{25}Mg was the mean of the cross sections deduced from the two prominent 585 and 975 keV transitions and is shown in Fig. 6. In addition to the experimental error, the final cross section for the channel contains a 10% error due to uncertainties in the calculation of the corresponding F factors. This estimate is consistent with the 10% deviation observed in Fig. 4, which contains the ratio R of calculated cross section for ^{25}Mg production when either the 585 keV yield or the 975 keV yield are used.

The cross section for the 585 keV transition in ^{25}Mg agrees very well with the results of Freeman[13] also shown as an average trend in Fig. 5. It disagrees, however, by a factor of 4 with the results of Chan *et al.*,[19] which in addition show marked structure in the cross section. These structures were not present in our experiment.

B. Two particle evaporation channels

Due to their moderate Q values (see Fig. 1), these channels contribute 90–95 % to the total fusion cross section. The strongest channels are ^{27}Al + p + n and ^{24}Mg + α + n, which account from 85% of the total cross section at low energies to 75% at the highest end of the

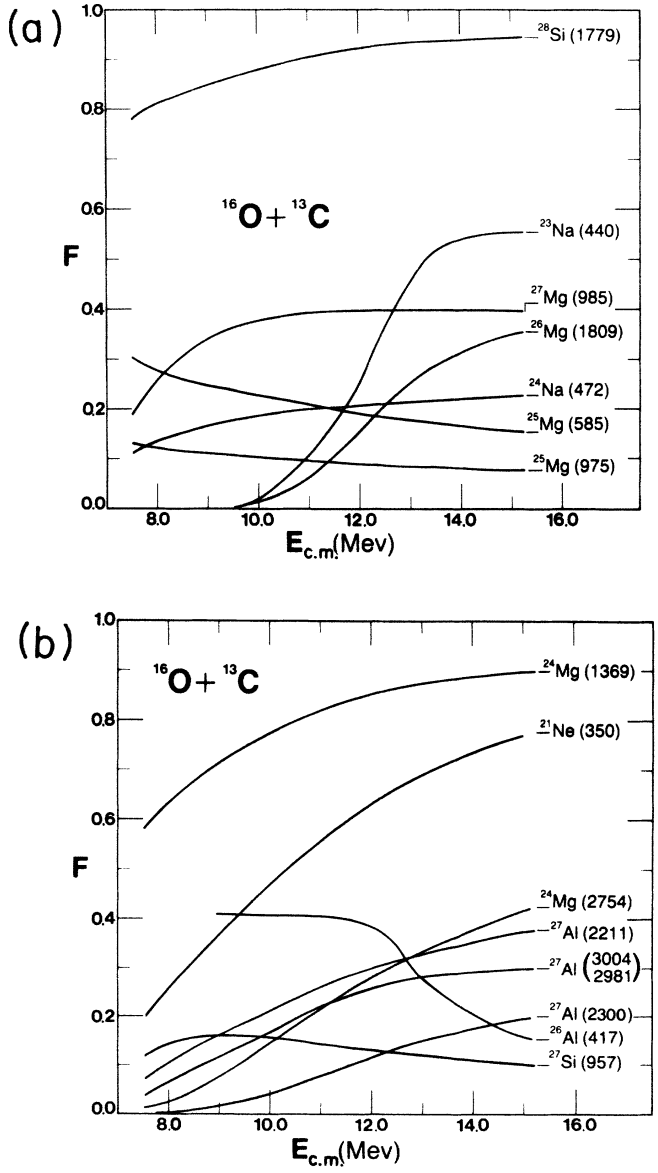

FIG. 3. Calculated summing and branching ratios for the γ rays employed in the reduction of the data.

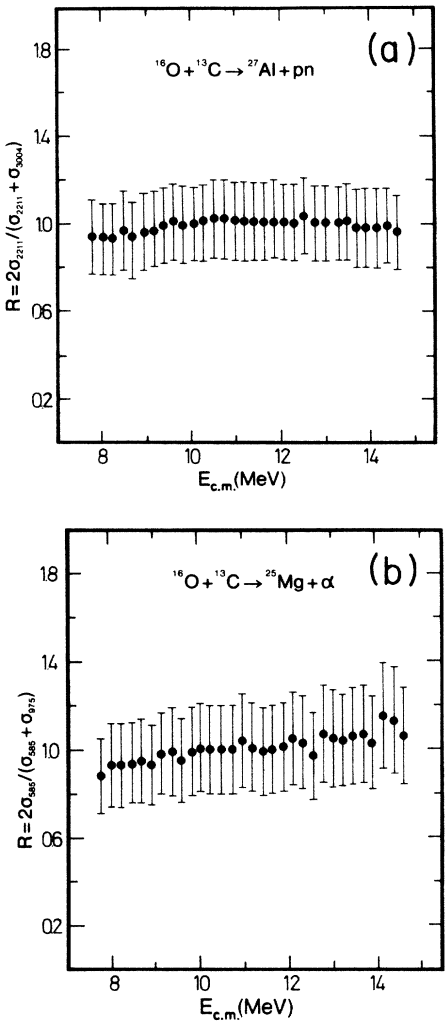

FIG. 4. The ratio of cross section estimates obtained from alternate γ rays for the population of ^{25}Mg and ^{27}Al in the reaction $^{16}O + ^{13}C$.

energy interval considered here. Each of these channels is discussed separately below.

$^{27}Si+n+n$. The cross section for this channel, shown in Fig. 6, was measured through the $\frac{3}{2}^+ \rightarrow \frac{5}{2}^+$, 957 keV transition in ^{27}Si. It is noted that the prediction of the statistical model, shown in the same figure, overestimates the experimental result by a factor of 2.

$^{27}Mg+p+p$. Figure 6 contains the cross section for this channel extracted from the 985 keV transition in ^{27}Mg. As seen from the figure these values agree within 20% with the cross section deduced from radioactivity measurements using the 844 and 1014 keV transitions in ^{27}Al, to which ^{27}Mg decays with a half-life of 9.5 min.

$^{27}Al+p+n$. A total of nine transitions were seen in this strongly populated channel. The cross sections measured for the three most prominent peaks are contained in Fig. 5. Contamination of these peaks by the $^{16}O + ^{12}C$ reaction was estimated as less than 2% and was ignored. The 2211 and 2300 keV γ-ray peaks, although exhibiting considerable Doppler broadening due to the short lifetimes of the corresponding initial states, were well separated and presented no problem in the analysis. This was not true for the 2981 and 3004 keV peaks which completely overlapped in the spectrum. These two peaks were therefore analyzed as one and the ratio R of the cross section for ^{27}Al calculated by either the 3004 + 2981 keV or the 2211 keV transitions is presented in Fig. 4 and shows negligible deviation from the expected value of unity.

$^{24}Mg+\alpha+n$. The prominent peak at 1369 keV after the necessary correction for contributions due to the β decay of ^{24}Na, was used in order to extract the cross section for this channel shown in Fig. 6. Contamination from the $^{16}O + ^{12}C$ reaction was again estimated as negligible. A second transition in ^{24}Mg at 2754 keV appears in the spectrum as a Doppler-shifted broad distribution covering a range of 80 keV. Although this distribution could be clearly separated from the corresponding unshifted peak, arising from the β decay of ^{24}Na, it covers several small peaks of various origins. This shows up in large deviations, especially at low energies, in the ratio R formed with the cross section of the 1369 keV γ ray. It was therefore not included in the calculation of the ^{24}Mg cross section shown in Fig. 6.

$^{24}Na+\alpha+p$. Only one transition at 472 keV was seen from this channel. A second transition at 1512 keV ($5^+ \rightarrow 4^+$), which is predicted in the statistical model calculation with considerable cross section, is not resolved due to interference with the 1506 keV transition in ^{27}Al. The cross section obtained for the 472 keV transition is shown in Fig. 5. It is noted that this channel is free from $^{16}O + ^{12}C$ contamination due to the large negative Q value for this reaction.

$^{21}Ne+\alpha+\alpha$. The cross section for this channel, shown in Fig. 6, was measured solely from the 350 keV transition in ^{21}Ne. The excitation function of the 350 keV transition is in excellent agreement with the one determined by Freeman[13] as shown in Fig. 5. On the other hand the experimental result for ^{21}Ne disagrees with the theoretical prediction within a factor of 4.

C. Three particle evaporation channels

The contribution to the total $^{16}O + ^{13}C$ fusion cross section from the three particle evaporation channels is extremely weak due to their considerably high negative Q values. In addition, all transitions attributed to these channels are heavily contaminated from $^{16}O + ^{12}C$ events which populate strongly the ^{26}Al, ^{26}Mg, ^{23}Na, and ^{20}Ne channels. An estimate of the cross section was possible only for the ^{26}Al channel.

$^{26}Al+p+n+n$. The cross section for populating this channel was estimated from the 417 keV γ-ray transition observed in the spectra. This peak was corrected for contributions from $^{16}O + ^{12}C$ events, which become important in the range of 10—14.6 MeV, resulting in an estimated 60% of the total number of counts at the highest energy. The corrected cross section from this transition, varying from 0.2 to 2 mb, is also included in Fig. 7. Due to the poor statistics of the corresponding peak and the uncertainty in the ^{12}C buildup through the run, the error associated with this data is considerable. In the reaction studied here the formation of ^{26}Al is expected mainly

through ^{26}Al + t (Q value −4.35 MeV) since the alternate channels (^{26}Al + d + n and ^{26}Al + p + n + n) open at higher energies (10.6 MeV and 12.8 MeV, respectively). This is born out in the data of Xenoulis *et al.*,[35] who studied this effect in the contamination-free ^{13}C + ^{16}O reaction. If the tritium contribution is included in the calculation, the F factor for the 417 keV transition in ^{26}Al, shown in Fig. 3, is obtained. This in turn leads to the ^{26}Al cross section, shown in Fig. 7, which ranges from 0.4 to 12 mb. The obtained absolute value agrees, within the experimental error, with the theoretical prediction, and contributes only about 1% to the total fusion cross section.

The ^{26}Mg, ^{23}Na, and ^{20}Ne channels. The γ rays which may arise from population of these channels are contained in Table I. If, however, the measured cross section[11] for ^{16}O + ^{12}C is employed in conjunction with the ^{12}C buildup through the run, all counts of the corresponding peaks in our spectra may be accounted for as due to contaminant events. This conclusion is corroborated by the Brookhaven[35] ^{13}C + ^{16}O coincidence data, where these

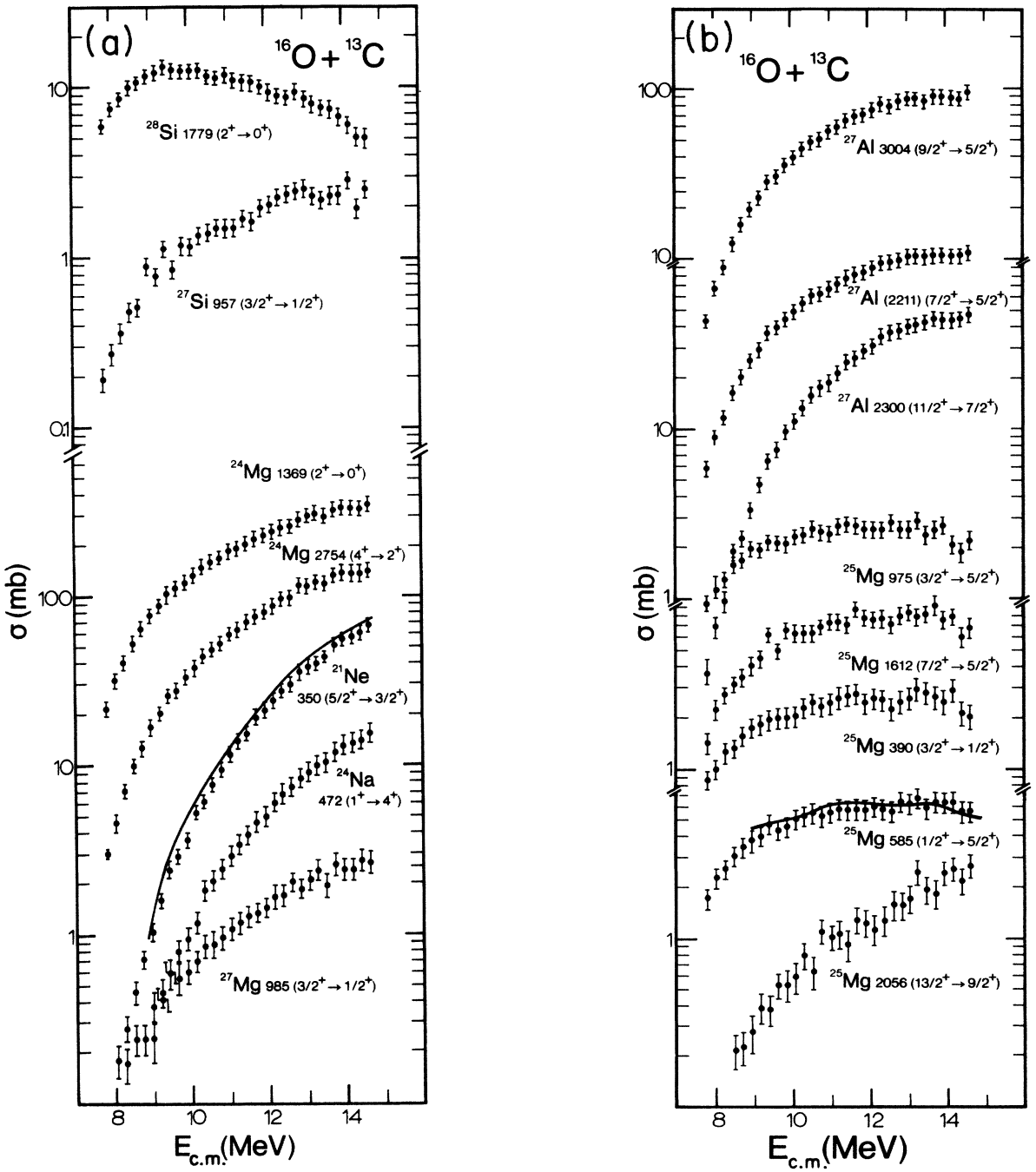

FIG. 5. Excitation functions for observed transitions in the final state of the reaction ^{16}O + ^{13}C. The continuous lines through the data in two transitions represent averaged measurements of the excitation function from the work of Freeman (Ref. 13).

peaks are not observed. Thus the contribution of these channels to the total fusion cross section was estimated only as an upper limit of 2%, and was included in the experimental error.

D. The one-neutron transfer channel

The γ-ray spectra obtained in this experiment permit in addition to the fusion evaporation processes described above, the study of peripheral channels like inelastic scattering and one-neutron transfer reactions. From the latter process the 871 keV transition in ^{17}O appears as a prominent peak in all spectra and yielded the excitation function in Fig. 8. It is noted that this peak may contain contamination from the 874 keV transition in ^{24}Na arising from the deexcitation of the 1346 keV level to the 472 keV level. However, by employing the observed intensity of the 472 keV ground-state transition, it was estimated that the contamination of the 871 keV peak ranged from a fraction of a percent up to 9% at the highest energy. This was taken into account in the excitation function presented in Fig. 8. Similarly, contributions from the 3α evaporation channel, which could be present in the data of Fig. 8, were considered negligible due to the high negative Q value for this channel ($Q=-8.08$ MeV) and from

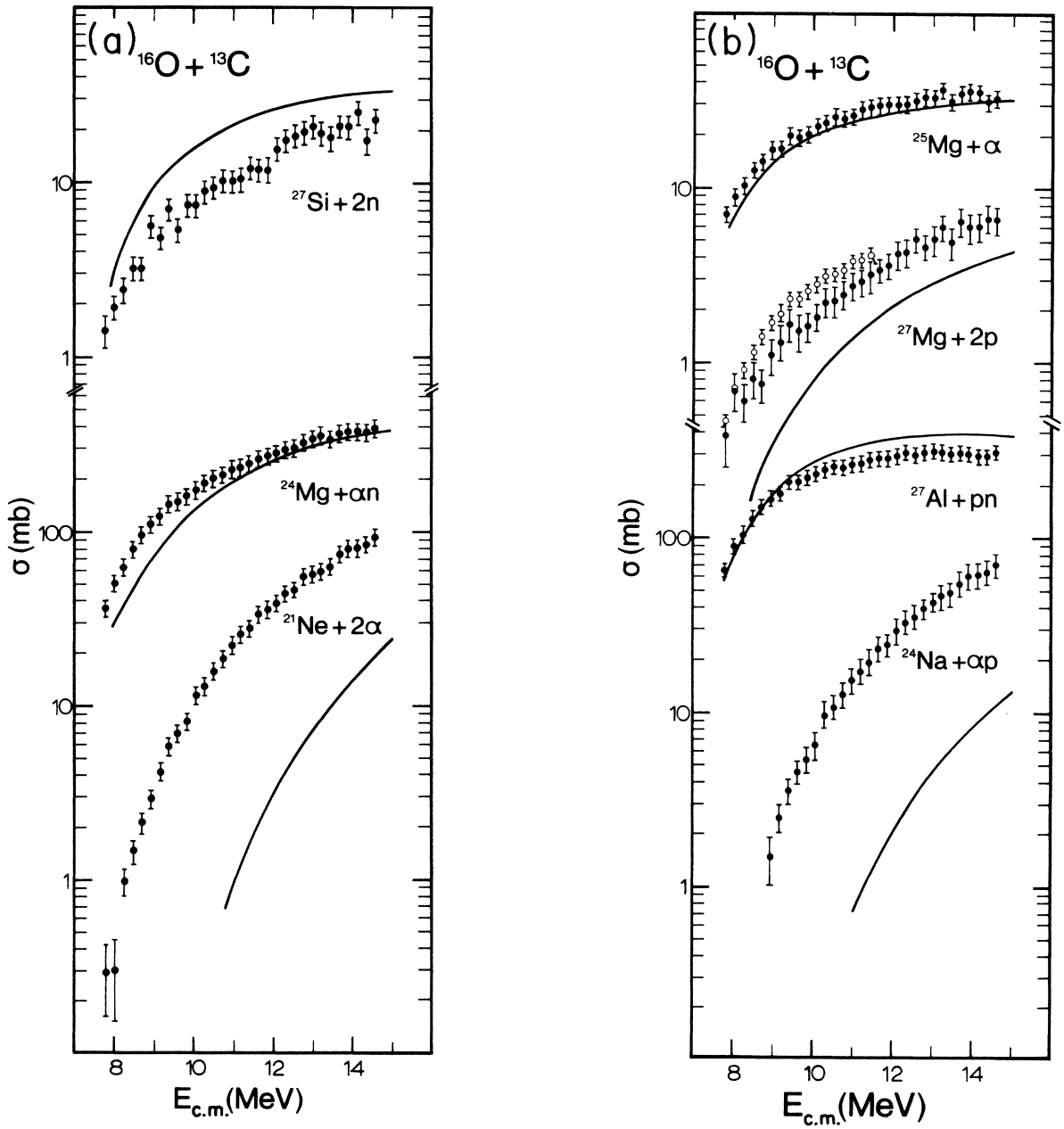

FIG. 6. Measured cross section for population of one and two particle evaporation channels in the reaction $^{16}O + ^{13}C$. Open circles represent results from activity measurements. The solid lines are the corresponding theoretical predictions from statistical model calculations.

Hauser-Feshbach calculations. The excitation function for the ^{17}O, 871 keV transition is compared in Fig. 8 with the data of Freeman[13] for the 871 and 874 keV transitions. The latter shows the same smooth trend while it systematically exceeds our results by approximately 20%.

The cross section measured for all evaporation channels populated by the reaction $^{16}O + ^{13}C$ are shown in Fig. 6. The errors associated with each measurement include (a) the statistical errors in the corresponding γ-ray peaks, (b) a 5% error in the determination of the absolute efficiency, (c) an 8% error arising from the normalization, and (d) a 5—10% error in the calculation of F factors. The solid curves in Fig. 6 represent the Hauser-Feshbach calculations using the same set of statistical model parameters as in the evaluation of the corresponding F factors.

The total fusion cross section, presented in Fig. 9, was obtained by summing the partial cross sections for all exit channels. The same figure contains the data of Dasmahapatra *et al.*[20] in the energy range 7.1—9.1 MeV, which are in fairly good agreement with the results presented here.

V. DISCUSSION

A. Statistical model calculations

The excitation functions for the fusion-evaporation products have been calculated in the framework of the Hauser-Feshbach theory using a modified version of the code STAPRE.[24] Numerical values of the parameters entering these calculations are the same as those employed in the evaluation of summing and branching factors, as described in Sec. II.

Statistical model calculations for the various exit channels are compared to the data in Fig. 6 and in general are seen to reproduce the overall trend of the excitation function. They seem, however, to overestimate the observed fusion cross section for neutron evaporation at the expense of flux for one or two alpha emission. Similar discrepancies have been observed in other systems[11,32,33] where the statistical model tends to underestimate the production of multiple α-particle evaporation channels.

An enhancement of the corresponding cross section may be affected by increasing the diffuseness of the entrance channel transmission coefficients. However, a change of the parameter $\hbar\omega$ in Eq. (3) from 3 to 5 MeV produces only a small change in this direction. In the same way, as described in Sec. III, variation of the level density parameters within limits of acceptable values were not able to account for this discrepancy.

B. Macroscopic treatment of the fusion cross section

In the "low energy" or barrier-dominated region (1 to 2 times the Coulomb barrier energy), the fusion cross section may be understood in terms of the penetrability of the ions through the interaction barrier, i.e., in terms of the interacting system's entrance channel characteristics. In this case the energy dependence of the fusion cross section is given by the relation

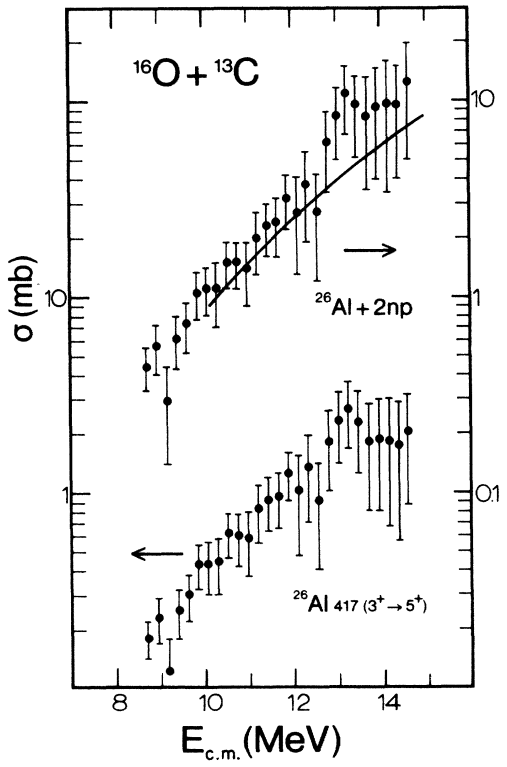

FIG. 7. Measured cross section in the $^{26}Al + p + n + n$ evaporation channel. The figure contains the cross section for the 417 keV transition (left scale) and the total channel cross section (right scale) estimated through Eq. (1). The solid line is the theoretical prediction from statistical model calculations.

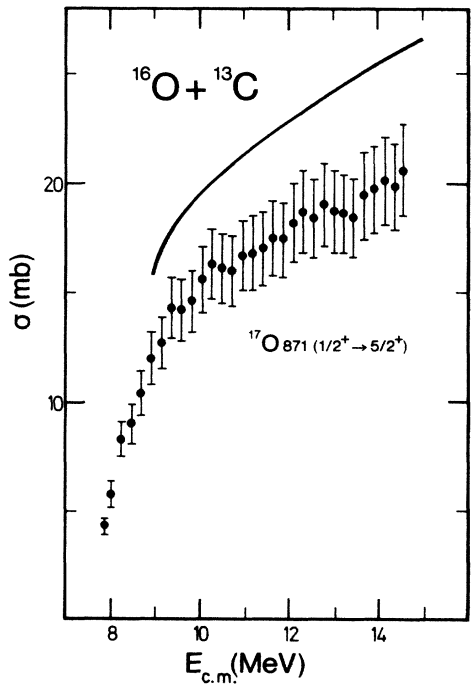

FIG. 8. Excitation function for the ^{17}O, 871 keV γ ray in the direct neutron transfer channel. The solid line represents the data of Freeman (Ref. 13), drawn as an average trend.

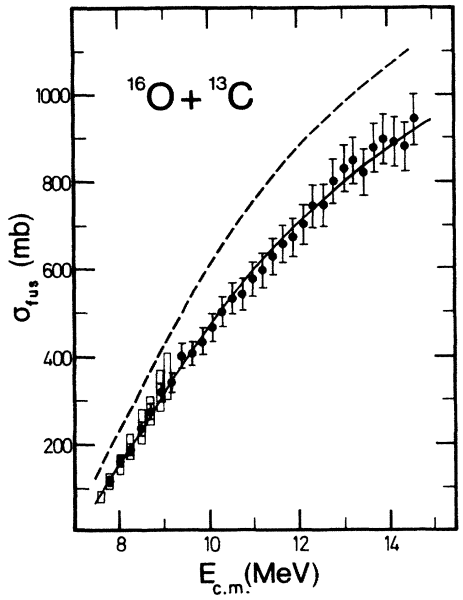

FIG. 9. Total fusion cross section of the $^{16}O + ^{13}C$ reaction. The low energy region contains also the data of Dasmahapatra *et al.* (Ref. 20). The continuous curves represent a macroscopic model fit (solid line) and the reaction cross section optical model calculation (dashed line), respectively.

$$\sigma_{fus}(E)=\pi\lambda\!\!\!^{-2}\sum_{l=0}^{\infty}(2l+1)T_l(E)P_l(E)\ , \tag{2}$$

where $\lambda\!\!\!^{-}$ is the incident wavelength, T_l the transmission coefficient for the lth incident wave, and P_l the probability of fusion for the corresponding incoming flux. In the region considered here P_l, to a very good approximation, may be taken equal to unity, due to the low relative velocity of the interacting nuclei as compared to the Fermi motion of the constituent nuclei.[36] The transmission coefficients T_l, entering Eq. (2), are given by the Hill-Wheeler expression

$$T_l(E)=\frac{1}{1+\exp[2\pi(V_{Bl}-E)/\hbar\omega_l]}\ , \tag{3}$$

where

$$V_{Bl}=V_B+\frac{\hbar^2 l(l+1)}{2\mu R_{Bl}^2} \tag{4}$$

is the height of the lth potential barrier, which occurs at the distance R_{Bl}, ω_l is the frequency of the inverted harmonic oscillator that approximates the lth barrier around R_{Bl}, and μ is the reduced mass of the interacting nuclei. It is noted that according to this expression the transmission coefficients T_l diminish rapidly to zero passed a given value of l, which depends on the specific values of parameters V_B, R_{Bl}, and ω_l. The summation in Eq. (3) may be thus conveniently terminated at a given value l_{max}, such that T_l becomes negligible for $l > l_{max}$.

By considering the parameters R_{Bl} and ω_l independent of l ($R_{Bl}=R_B$, $\omega_l=\omega$) and replacing the summation by integration, Wong[1] has derived a simple expression for the fusion cross section

$$\sigma_{fus}(E)=\frac{R_B^2\hbar\omega}{2E}\ln\{1+\exp[2\pi(E-V_B)/\hbar\omega]\}\ . \tag{5}$$

For $E > V_B$ this simplifies further into the expression

$$\sigma_{fus}(E)=\pi R_B^2\left[1-\frac{V_B}{E}\right] \tag{6}$$

which, however, as pointed out by Nagatani *et al.*,[36] may constitute an unacceptably crude approximation.

Numerical values of the barrier penetration parameters for the $^{16}O+^{13}C$ system were obtained by fitting the fusion cross section measured here with the above analytic expressions. Three different fits to the data were performed:

(a) Through Eq. (2), by considering the parameters R_B and ω independent of l and extending the summation up to a value l_{max}, with $T_l < 0.01$ for $l > l_{max}$.
(b) Through the Wong approximation in Eq. (5).
(c) Through the simple expression of Eq. (6) for energies greater than 1.1 times the Coulomb barrier.

In all three cases the fit, shown in Fig. 9, produces practically identical results, yielding numerical values for the barrier parameters

$$\begin{aligned} R_B &= 7.7\pm0.1 \text{ fm}\ , \\ V_B &= 7.5\pm0.1 \text{ MeV}\ , \\ \hbar\omega &= 3.0\pm0.7 \text{ MeV}\ . \end{aligned} \tag{7}$$

These values also coincide, within experimental errors, with those obtained for the adjacent system[12] $^{16}O + ^{12}C$. It is therefore concluded that the three-parameter macroscopic treatment of the fusion cross section presented above does not contain adequate sensitivity in order to distinguish the presence of the additional nucleon in the interacting system. This lack of sensitivity is also borne out by the comparison of our fusion cross section with the corresponding data for the $^{16}O + ^{12}C$ system, as presented in the compilation of Kovar *et al.*[12] Indeed the significant enhancement of the $^{16}O + ^{13}C$ system over $^{16}O + ^{12}C$, observed by Dasmahapatra *et al.*[20] at energies below the Coulomb barrier, seems to gradually disappear, within experimental errors, in the energy range considered here.

In a more refined version of the macroscopic approach, the l dependence of the barrier penetration parameters entering Eqs. (2)–(4) may be considered. Following the treatment of Vaz *et al.*,[38] we have considered a proximity potential.[39] In this calculation the sharp radii $R_i=1.28A_i^{1/3}-0.76+0.8Z_i^{1/3}$ of the two colliding nuclei were varied by an amount ΔR in order to improve the agreement between theory and experiment. The best fit was obtained for $\Delta R=0.23$ fm which leads to a radius $R_{Bo}=8.2$ fm and height $V_{Bo}=7.7$ MeV for the $l=0$ barrier. It should be noted that this change in the nuclear radius that needed to fit the experimental data exceeds by far the uncertainties due to the liquid-drop model derivation of the nuclear radius.[40] On the other hand the values

TABLE III. Parameters employed in empirical model calculations of the fusion cross section for $^{16}O + ^{13}C$.

b (fm)	c	d	m (fm/MeV)	Proposed by
8.93	18	2.33	−0.0660	Horn and Ferguson (Ref. 41)
9.28	21	2.44	−0.0753	Lozano and Madurga (Ref. 42)
10.51	21	2.80	−0.1749	Present work

obtained for the radius and height of the s-wave potential are similar to those reported by Vaz and Alexander[38] for adjacent systems.

C. Empirical model parametrization

In order to take into account the nuclear structure of the colliding ions, a parametrization of the fusion cross section, initially proposed by Horn and Ferguson,[41] may be employed. In this model the fusion cross section is written as

$$\sigma_{\text{fus}}(E_{\text{c.m.}}) = \pi\rho^2 \left[1 - \frac{D}{\rho}\right], \tag{8}$$

$$D = \frac{Z_1 Z_2 e^2}{E}, \tag{9}$$

where the fixed parameter R in Eq. (6) is given the energy dependence

$$\rho = mE_{\text{c.m.}} + b. \tag{10}$$

In the last equation b is the sum of the radii of the two interacting nuclei at a given percentage level of their central charge density (1.35% according to Ref. 41) and m is evaluated through the empirical relation

$$m^{-1} = c(d - A_{\text{CN}}^{1/3}), \tag{11}$$

where c and d are parameters with numerical values deduced from fusion cross section systematics. In the initial proposal of Horn and Ferguson the values $c=18$ and $d=2.23$ resulted in a satisfactory reproduction of the fusion excitation function in a wide range of interacting systems.

More recently Lozano and Madurga[42] have modified this model by considering nuclear densities rather than charge densities for the definition of the parameter b. The corresponding values of the parameters entering Eq. (11) proposed by these authors, are $c=21$ and $d=2.44$.

The predictions of both types of parameterization of the fusion cross section described above are shown in Fig. 10. Above 10 MeV the parameterization of Lozano and Madurga is in fairly good agreement with the data. The values of the parameters employed in these calculations are summarized in the first two entries of Table III. As a further test of this empirical model, however, an alternate process was investigated according to which Eqs. (8)—(11) were fitted to the experimental data by treating parameters b, c, and d as free parameters. The best fit obtained through this process is also included in Fig. 10 (solid line), while the corresponding values of the parameters are contained in the third entry of Table III. This procedure produced only a marginally improved fit compared to the Lozano and Madurga parametrization. It is noted that the value of the distance b obtained in this fashion corresponds to the sum of ^{13}C and ^{16}O radii at 0.12% of the charge density.

D. Optical model analysis

In order to test whether the total reaction cross section for the $^{16}O + ^{13}C$ system may be accounted for by the fusion cross section measured here, an optical model analysis was performed on the elastic scattering data of Gobbi *et al.*[43] The analysis was carried out with the automatic search code ATHREE,[44] by assuming a standard Woods-Saxon potential for both the real and imaginary parts, specially suited to heavy ion calculations. Using the optical model parameters obtained by Michaud[45] for the $^{16}O + ^{12}C$ system as starting values, the results contained in Table IV were reached. Values of the parameters in the rest of the energy range covered by the present experiment were taken by smooth extrapolation of the results contained in Table IV. The reaction cross section calculated in this fashion is also contained in Fig. 9 and is seen to overestimate the measured fusion cross section by approximately 20%. This difference is consistent with the expected contribution of the direct neutron transfer in the reaction cross section.

E. Gross structure in the excitation function

None of the measured excitation functions for the $^{16}O + ^{13}C$ system presents evidence of structures in the energy range covered here. Such structure would be expected particularly in the α-evaporation channels (due to the larger angular momentum carried by the heavier parti-

TABLE IV. Optical model parameters obtained from elastic scattering data (Ref. 43) in the $^{16}O + ^{13}C$ system

$$V_{\text{op}}(r) = (V + iW)\frac{1}{1 + \exp\left[\dfrac{r-R}{\alpha}\right]},$$

$$R = r(A_1^{1/3} + A_2^{1/3}).$$

$E_{\text{c.m.}}$ (MeV)	V (MeV)	W (MeV)	α (fm)	r (fm)	R	σ_R (mb)
8.39	60	2.8	0.37	1.46	7.11	312
9.42	57	3.7	0.45	1.36	6.62	512
10.44	64	4.5	0.55	1.26	6.14	680

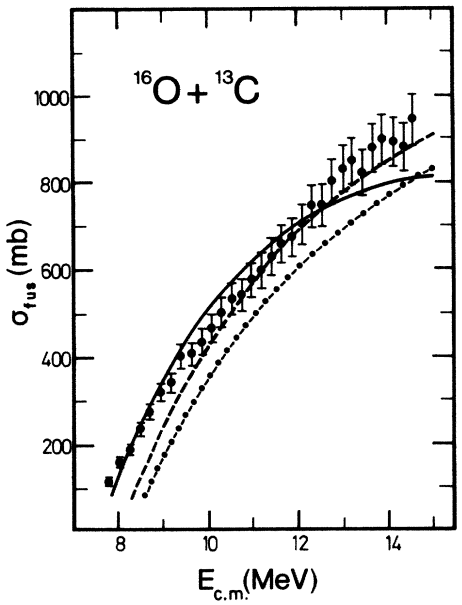

FIG. 10. Total fusion cross section of the $^{16}O + ^{13}C$ reaction. The continuous curves represent (a) an empirical model fit through the parametrization of Eqs. (8)—(11) (solid line), (b) prediction of the Lozano-Madurga model (dashed line), and (c) prediction of the Horn-Ferguson model (dashed-dotted line).

cles) and more pronounced for transitions emanating from high spin states. In the first study of the $^{16}O + ^{13}C$ system, Chan *et al.*[19] reported evidence of structure in the excitation function for the deexcitation of the 585 keV $\frac{1}{2}^+$ state of ^{25}Mg in the single α evaporation channel. This was not, however, reproduced in the experiment of Freeman.[13] On the other hand, should structure exist in the excitation function for this transition, it should also appear, more pronounced, in the 2056 keV transition emanating from a $\frac{13}{2}^+$ state of ^{25}Mg. Although this γ ray carries a very small part of the cross section in the single α evaporation channel, the corresponding peak in the spectra was well formed due to the large lifetime (2.5 ps) of the parent 5462 keV, $\frac{13}{2}^+$ state. The resulting excitation function, included in Fig. 5, showed no evidence of structure.

An alternate candidate for the observation of oscillatory behavior is the excitation function of the $^{17}O + ^{12}C$ single neutron transfer channel. Recently, Freeman *et al.*[46] have observed a marked structure in the excitation curve of the 871 keV γ ray of ^{17}O arising from inelastic scattering in $^{13}C + ^{17}O$. Abe and Park[47] have suggested an explanation of this structure in terms of the Landau-Zener excitation mechanism at energy level crossings, while Park *et al.*[48] have proposed the $^{16}O + ^{13}C$ and $^{17}O + ^{12}C$ systems as possible candidates for similar behavior in the neutron transfer and inelastic channels. The excitation function for the 871 keV γ ray of ^{17}O, arising from the neutron transfer reaction in $^{16}O + ^{13}C$, measured in this work, is presented in Fig. 8. In the energy range covered here the excitation function is seen to be devoid of any structure. This is in accordance with recent preliminary data of the Strasbourg group,[13] which cover the more extended energy range of 9—22 MeV.

VI. CONCLUSIONS

The cross section for populating evaporation channels and the total fusion cross section in the $^{16}O + ^{13}C$ system have been measured through the observation of singles γ rays. In the center of mass energy range 7.8—14.6 MeV examined here, the enhancement of the total fusion cross section over the $^{16}O + ^{12}C$ system, reported by Dasmahapatra *et al.*[20] at lower energies, seems to gradually disappear with increasing energy. The excitation functions for both total and individual channel cross section are devoid of any structure in contrast with the well-known prominent oscillations observed in $^{16}O + ^{12}C$. This may be attributed to the loosely bound valence neutron ($Q = -4.95$ MeV) in the ^{13}C nucleus. The same smooth behavior is observed for the ^{17}O, 871 keV γ ray in the direct n-transfer channel, although some structure was anticipated[48] in the framework of the Landau-Zener effect. The overall trend of the excitation functions measured here was satisfactorily accounted for by statistical model calculations. These calculations, as usually observed,[11,32,33] however, seem to overestimate the measured cross section for neutron evaporation channels at the expense of flux for one or multiple alpha emission.

While this paper was being concluded, a paper by Beck *et al.*[49] of the Strasbourg group appeared in the literature, which essentially reports the completed investigation of the $^{17}O + ^{12}C$ and $^{16}O + ^{13}C$ systems, presented in Ref. 13 as preliminary data. These authors have measured excitation functions for the seven most prominent γ rays in $^{16}O + ^{13}C$ between 20 and 70 MeV laboratory energy. In the overlapping energy range the data of Beck *et al.*[49] seem to coincide with the results presented here.

The authors are grateful to the Gesellschaft für Schwerionenforschung Darmstadt Institute and in particular to Dr. Dieter Schardt for providing the ^{13}C target.

[1]C. Y. Wong, Phys. Lett. **42B**, 186 (1972); Phys. Rev. Lett. **31**, 766 (1973).

[2]D. Glass and U. Mosel, Phys. Rev. C **10**, 2620 (1974); Nucl. Phys. **A237**, 429 (1975).

[3]M. Lefort, Phys. Scr. **10A**, 101 (1974).

[4]S. M. Lee, T. Matsuse, and A. Arima, Phys. Rev. Lett. **45**, 165 (1980).

[5]*Proceedings of the International Conference on the Resonant Behavior of Heavy-Ion Systems, Aegean Sea, Greece, 1980,* edited by G. Vourvopoulos (Nuclear Research Center "Democritos," Athens, 1981).

[6]P. Sperr, T. H. Braid, Y. Eisen, D. G. Kovar, F. W. Prosser, Jr., J. P. Schiffer, S. L. Tabor, and S. Vigdor, Phys. Rev. Lett. **37**, 321 (1976).

[7]M. Conjeaud, S. Gary, S. Harar, and J. P. Wieleczko, Nucl. Phys. **A309**, 515 (1978).
[8]B. Fernandez, C. Gaarde, J. S. Larsen, S. Pontoppidan, and F. Videbaek, Nucl. Phys. **A306**, 259 (1978).
[9]P. Sperr, S. Vigdor, Y. Eisen, W. Henning, D. G. Kovar, T. R. Ophel, and B. Zeidman, Phys. Rev. Lett. **36**, 405 (1976).
[10]R. M. Freeman, F. Haas, B. Heusch, and A. Gallmann, Phys. Rev. C **19**, 408 (1979).
[11]Y. D. Chan, H. Bohn, R. Vandenbosch, K. G. Bernhardt, J. E. Cramer, R. Sielemann, and L. Green, Nucl. Phys. **A303**, 500 (1978).
[12]D. G. Kovar, D. F. Geesaman, T. H. Braid, Y. Eisen, W. Henning, T. R. Ophel, M. Paul, K. E. Rehm, S. J. Sanders, P. Sperr, J. P. Schiffer, S. L. Tabor, S. Vigdor, and B. Zeidman, Phys. Rev. C **20**, 1305 (1979).
[13]R. M. Freeman, in Ref. 5, p. 41.
[14]J. P. Wieleczko, S. Harar, M. Conjeaud, and F. Saint-Laurent, Phys. Lett. **93B**, 35 (1980).
[15]Y. Eyal, M. Beckerman, R. Cheehik, Z. Fraenkel, and H. Stocker, Phys. Rev. C **13**, 1527 (1976).
[16]A. Hertz, H. Essel, H. J. Körner, K. E. Rehm, and P. Sperr, Phys. Rev. C **18**, 2780 (1978).
[17]R. M. Freeman, F. Haas, and V. Korschinek, Phys. Lett. **90B**, 229 (1980).
[18]R. M. Freeman and F. Haas, Phys. Rev. Lett. **40**, 927 (1978).
[19]Y.-d. Chan, H. Bohn, R. Vandenbosch, R. Sielemann, J. G. Cramer, K. G. Bernhardt, H. C. Bhang, and D. T. Chiang, Phys. Rev. Lett. **40**, 687 (1979).
[20]B. Dasmahapatra, B. Ĉujec, and F. Lahlou, Nucl. Phys. **A394**, 301 (1983).
[21]K. Alder, A. Bohr, T. Huus, B. Mottelson, and A. Winther, Rev. Mod. Phys. **28**, 432 (1956).
[22]P. R. Sharma, Nucl. Phys. **A154**, 312 (1970).
[23]Z. E. Switkowski, R. G. Stokstad, and R. M. Wieland, Nucl. Phys. **A274**, 202 (1976).
[24]M. Uhl, Acta Phys. Austriaca **31**, 245 (1970).
[25]P. M. Endt and C. Van der Leun, Nucl. Phys. **A310**, 1 (1978).
[26]H. K. Vonach and I. Hille, Nucl. Phys. **A127**, 289 (1969).
[27]D. W. Lang, Nucl. Phys. **77**, 545 (1966).
[28]D. Wilmore and P. E. Hodgson, Nucl. Phys. **55**, 673 (1964).
[29]F. G. Perey, Phys. Rev. **131**, 745 (1963).
[30]C. M. Perey and F. G. Perey, Phys. Rev. **132**, 755 (1963).
[31]J. R. Huizenga and G. Igo, Nucl. Phys. **29**, 462 (1961).
[32]J. L. Charvet, R. Dayras, J. M. Fieni, S. Joly, and J. L. Uzureau, Nucl. Phys. **A376**, 292 (1982).
[33]J. Dauk, K. P. Lieb, and A. M. Kleinfeld, Nucl. Phys. **A241**, 170 (1975).
[34]A. C. Xenoulis, E. N. Gazis, P. Kakanis, D. Bucurescu, and A. D. Panagiotou, Phys. Lett. **90B**, 224 (1980); D. Bucurescu, private communication.
[35]A. C. Xenoulis, A. E. Aravantinos, C. J. Lister, J. W. Olness, and R. L. Kozub, Phys. Lett. **106B**, 461 (1981).
[36]K. Nagatani and J. C. Peng, Phys. Rev. C **19**, 747 (1979).
[37]D. L. Hill and J. A Wheeler, Phys. Rev. **89**, 1102 (1953).
[38]L. C. Vaz and J. M. Alexander, Phys. Rev. C **18**, 2152 (1978); L. C. Vaz, J. M. Alexander, and G. R. Satchler, Phys. Rep. **69**, 373 (1981).
[39]J. Blocki, J. Randrup, W. J. Swiatecki, and C. F. Tsang, Ann. Phys. (N.Y.) **105**, 427 (1977).
[40]W. D. Myers, Nucl. Phys. **A204**, 465 (1973).
[41]D. Horn and A. J. Ferguson, Phys. Rev. Lett. **41**, 1529 (1978).
[42]M. Lozano and G. Madurga, Phys. Lett. **90B**, 50 (1980).
[43]A. Gobbi, U. Matter, T. L. Perrenoud, and P. Marmier, Nucl. Phys. **A112**, 537 (1968).
[44]E. H. Auerbach, Comput. Phys. Commun. **15**, 165 (1978).
[45]G. J. Michaud and F. W. Vogt, Phys. Rev. C **5**, 350 (1972); G. Michaud, *ibid.* **8**, 525 (1973).
[46]R. M. Freeman, C. Beck, F. Haas, B. Heusch, and J. J. Kolata, Phys. Rev. C **28**, 437 (1983).
[47]Y. Abe and J. Y. Park, Phys. Rev. C **28**, 2316 (1983).
[48]J. Y. Park, W. Greiner, and W. Scheid, Phys. Rev. C **21**, 958 (1980).
[49]C. Beck, R. M. Freeman, F. Haas, and B. Heusch, Nucl. Phys. **A443**, 157 (1985).